

Extended emission and spectral break in Cen A

Volker Beckmann*

François Arago Centre, APC, Université Paris Diderot, CNRS/IN2P3, CEA/DSM, Observatoire de Paris, 13 rue Watt, 75205 Paris Cedex 13, France

E-mail: beckmann@apc.univ-paris7.fr

Pierre Jean

Centre d'Étude Spatiale des Rayonnements (CESR), OMP, UPS, CNRS; B.P. 44346, 31028 Toulouse Cedex 4, France

Piotr Lubiński

Centrum Astronomiczne im. M. Kopernika, Rabiańska 8, PL-87-100 Toruń, Poland

Simona Soldi

Laboratoire AIM - CNRS - CEA/DSM - Université Paris Diderot (UMR 7158), CEA Saclay, DSM/IRFU/SaP, 91191 Gif-sur-Yvette, France

Regis Terrier

APC, Université Paris Diderot, CNRS/IN2P3, CEA/DSM, Observatoire de Paris, 75013 Paris

The radio galaxy Cen A has been detected all the way up to the TeV energy range. This raises the question about the dominant emission mechanisms in the high-energy domain. Spectral analysis allows us to put constraints on the possible emission processes. Here we study the hard X-ray emission, in order to distinguish between a thermal or non-thermal inverse Compton process. The hard X-ray spectrum of Cen A shows a significant cut-off at energies $E_C = 434^{+109}_{-74}$ keV with an underlying power law of photon index $\Gamma = 1.73 \pm 0.02$. A more physical model of thermal Comptonisation (compPS) gives a plasma temperature of $kT_e = 206 \pm 62$ keV within the optically thin corona with Compton parameter $y = 0.42^{+0.09}_{-0.06}$. The reflection component is significant at the 3.6σ level with $R = 0.12^{+0.09}_{-0.10}$. Extending this model to the gamma-ray range shows that a different physical component is responsible for the high-energy emission. The analysis of the SPI data provides no sign of significant emission from the radio lobes and gives a 3σ upper limit of $f_{40-1000\text{keV}} < 1.1 \times 10^{-3} \text{ ph cm}^{-2} \text{ s}^{-1}$. We find though some indication of emission near to the northern lobe of Cen A which we investigate in more detail.

8th INTEGRAL Workshop "The Restless Gamma-ray Universe"

September 27-30 2010

Dublin Castle, Dublin, Ireland

*Speaker.

1. Introduction

The radio galaxy Centaurus A (NGC 5128) is probably the best studied active galactic nucleus (AGN). With a redshift of $z = 0.001825$ equivalent to a distance of $d \sim 3.5$ Mpc the object is the brightest AGN at hard X-rays with $f_{20-100\text{keV}} \simeq 6 \times 10^{10} \text{ erg cm}^{-2} \text{ s}^{-1}$ [1]. For a review on Cen A, see [2]. Early hard X-ray observations by *Ginga* and balloon borne detectors indicated a power law slope of $\Gamma \sim 1.8$ and a possible break at ~ 180 keV [3]. The *Compton Gamma-Ray Observatory's* (CGRO; [4]) OSSE and COMPTEL instruments derived a more complex structure with a two-fold broken power law, with breaks at $E_1 = 150_{-20}^{+30}$ keV and at $E_2 = 17_{-16}^{+28}$ MeV [5]. More recent *RXTE* and *INTEGRAL* observations showed an absorbed un-broken power law with photon index $\Gamma \simeq 1.8$ and an intrinsic hydrogen column density of $N_{\text{H}} \simeq 10^{23} \text{ cm}^{-2}$ [6, 7]. Nevertheless, Cen A shows a steeper spectral slope in the MeV range ($\Gamma_{\gamma} = 2.3 \pm 0.1$, [8]) than in the hard X-rays ($\Gamma_{\text{X}} \ll 2$), thus a turnover has to occur somewhere between 100 keV and a few MeV [9]. The source was also the only non-blazar AGN detected by *CGRO/EGRET* [10], showing again a steepening of the spectrum with $\Gamma_{0.03-10\text{GeV}} = 2.4 \pm 0.3$ [11], consistent with the recent observations by *Fermi/LAT* ($\Gamma = 2.7 \pm 0.1$, [12]) and extending up to the TeV range, as seen by the *HESS* experiment ($\Gamma_{E>100\text{GeV}} = 2.7 \pm 0.5$, [13]). *Fermi/LAT* observations also discovered extended gamma-ray emission which co-incides with the radio lobes [14].

The multi-year database of the *INTEGRAL* mission allows now to search the hard X-ray spectrum of Cen A for the expected turnover. In addition, we can test whether the emission model applicable for the X-ray domain can also explain the emission at gamma-rays.

2. Data analysis

In this study we use all *INTEGRAL* data on Cen A taken between March 3, 2003 and February 21, 2009, i.e. all observations dedicated to this radio galaxy. We used data of the imager IBIS/ISGRI in the 20–1000 keV band, IBIS/PICsIT data at 234 – 632 keV, and those of the spectrometre SPI between 40 keV and 1850 keV. The two JEM-X monitors provide spectral information in the 3 – 30 keV band. We selected the data up to an off-axis angle of 10° for IBIS/ISGRI and SPI, and within 3° for JEM-X. Data reduction was performed using the Offline Scientific Analysis (OSA) package version 9.0. The PICsIT data analysis followed the procedure described in Lubinski et al. [15]. The different instruments were not always switched on simultaneously. The effective exposure times are therefore different, with 145 ks for JEM-X1, 96 ks JEM-X2, 1,425 ks IBIS/ISGRI, 2,076 ks IBIS/PICsIT, and 1,858 ks for SPI.

Errors quoted in this work are at the 3σ level.

3. The hard X-ray spectrum

For spectral analysis we added all *INTEGRAL* data together, i.e. JEM-X1, JEM-X2, SPI, IBIS/PICsIT, and IBIS/ISGRI. A simple absorbed power law ($\Gamma = 1.85 \pm 0.01$) does not provide a good representation of the data ($\chi_{\nu}^2 = 1.83$, 104 d.o.f.). An absorbed cut-off power law model gives $\chi_{\nu}^2 = 1.07$ (103 d.o.f.) with a photon index of $\Gamma = 1.73 \pm 0.02$ and $E_C = 434_{-74}^{+109}$ keV. The spectral shape and the cut-off energy are not independent variables. A flatter spectrum is compensated in

Table 1: Spectral fits to combined *INTEGRAL* data. All errors are at the 3σ level.

| model | Γ | E_C or kT_e [keV] | y | R | χ^2_{ν} (d.o.f.) |
|---------|-----------------|--------------------------|------------------------|------------------------|-------------------------|
| power | 1.85 ± 0.01 | – | – | – | 1.83 (104) |
| cut-off | 1.73 ± 0.02 | 434^{+109}_{-74} | – | – | 1.07 (103) |
| pextrav | 1.75 ± 0.04 | 549^{+387}_{-168} | – | $0.07^{+0.11}_{-0.07}$ | 1.07 (102) |
| compPS | – | 206 ± 62 | $0.42^{+0.09}_{-0.06}$ | $0.12^{+0.08}_{-0.10}$ | 1.02 (101) |

the fit by a lower cut-off energy. Nevertheless, a cut-off energy below 300 keV and above 700 keV can be ruled out at a 99.7% confidence level. The spectral slope is better constrained by the data spanning 3 – 1000 keV. Even when considering different cut-off energies, the 3σ range for the photon index is $1.68 < \Gamma < 1.78$.

The cut-off power law is a phenomenological description of the spectrum. A physical model should include the processes of thermal Comptonization. Here we apply the `compPS` model [16]. We assume that the plasma of temperature T_e forms an infinite slab on top of the accretion disk, with the plasma having an optical depth τ . Since T_e and τ are intrinsically strongly anticorrelated, we fit the Compton parameter $y = 4\tau kT_e / (m_e c^2)$ (with m_e being the electron mass) instead of the optical depth. The temperature of the seed photons is not well constrained by the hard X-ray spectrum used here, thus we assume a multicolor disk with a fixed inner temperature $T_{bb} = 10$ eV.

The `compPS` model gives an electron plasma temperature of $kT_e = 206 \pm 62$ keV, and a Compton parameter $y = 0.42^{+0.09}_{-0.06}$ corresponding to an optical depth of $\tau = 0.26$ ($\chi^2_{\nu} = 1.02$ for 101 d.o.f.). In this fit, we had to let the plasma temperature of the PICsIT spectrum to be independent from the other instruments, as the PICsIT spectrum appears slightly harder. This results for the PICsIT spectrum in a temperature as high as 675 keV, which cannot be constrained by the fit. The reflection strength is $R = 0.12^{+0.08}_{-0.10}$, inconsistent with no reflection at the 3.6σ level. Similar to the tight connection between the cut-off energy and the underlying spectral slope in the case of the cut-off power law model, in the `compPS` model the plasma temperature T_e and the Compton parameter y are linked to each other. Considering all combinations, the plasma temperature range is very wide ($300 \text{ keV} > kT_e > 100 \text{ keV}$) with a Compton parameter $0.34 < y < 0.57$ corresponding to a range of optical depth $0.14 < \tau < 0.69$.

The average model flux in the X-rays as detectable by *INTEGRAL* is $f_{(3-1000 \text{ keV})} = 3 \times 10^{-9} \text{ erg cm}^{-2} \text{ s}^{-1}$, and thus Cen A displays a luminosity of $L_X = 2.2 \times 10^{43} \text{ erg s}^{-1}$.

For comparison we applied the more simple `pextrav` model which describes an exponentially cut-off power law spectrum reflected from neutral material, with the output spectrum being the sum of the cut-off power law and the reflection component [17]. In this case the best fit results ($\chi^2_{\nu} = 1.07$ for 102 d.o.f.) are a photon index of $\Gamma = 1.75 \pm 0.04$, cut-off energy $E_C = 549^{+387}_{-168}$ keV and relative reflection of $R = 0.07^{+0.11}_{-0.07}$, consistent with no reflection.

All the fit results concerning the combined *INTEGRAL* spectrum are summarized in Table 1.

4. Extended emission

As a radio galaxy, Cen A (RA = 201.3651°, DEC = −43.0191°) is known to have radio

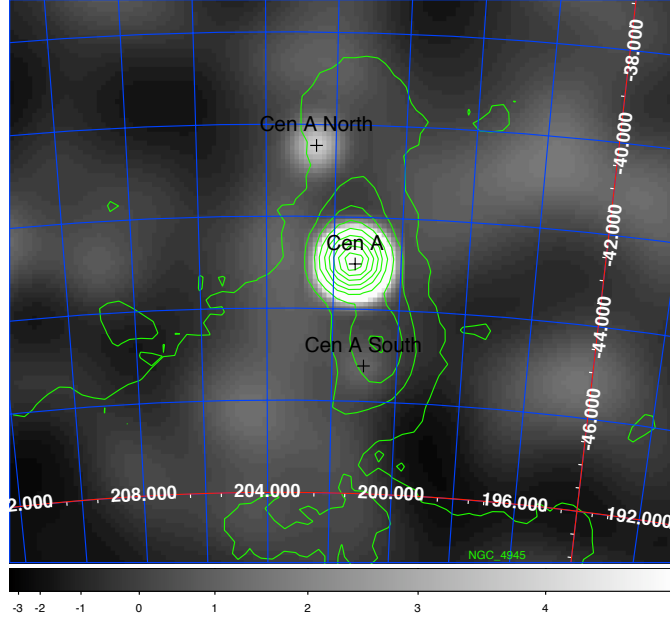


Figure 1: *INTEGRAL*/SPI significance map in the 40 – 1000 keV energy band of the Cen A region. Overlaid are the contours of the WMAP radio map. Note that the hard X-ray emission of the lobes is not significant.

lobes extending out from the core by about 300 kpc. These lobes are located in the north at RA= 201.5°, DEC = −39.8° and in the south at RA = 200.625°, DEC = −44.716°. Recently, *Fermi*/LAT detected emission from positions consistent with these lobes at significance levels of 5 σ (1FGL J1333.4–4036) and 8 σ (1FGL J1322.0–4545) for the northern and southern lobes, respectively [14]. Here we use the data of the spectrometre SPI to test for emission of the lobes at hardest X-rays. Because of its large field of view and a resolution of 2.5', SPI is able to map large scale structures on the hard X-ray background. The spectra of the radio lobes and Cen A were extracted by model fitting, assuming that the sky intensity distribution consist of these 3 point sources, at the positions mentioned above. We performed the analysis in 10 keV wide energy bins, covering the 40–1850 keV range. Each energy bin is adjusted to the data for each germanium detector separately, assuming that the count rate is due to the sum of the sky contributions and the instrumental background. The latter is assumed to be proportional to the rate of saturating events in germanium detectors [18]. The spectra were rebinned in logarithmic spaced energy bins for the spectral analysis presented in Section 3. The analysis of the SPI data shows no sign of significant emission from the radio lobes in the south (3 σ upper limit $f_{40-1000\text{keV}} < 1.1 \times 10^{-3} \text{ ph cm}^{-2} \text{ s}^{-1}$) and in the north with $f = 1.0 \pm 0.4 \times 10^{-3} \text{ ph cm}^{-2} \text{ s}^{-1}$ for a non-significant signal on the 2.5 σ level.

We investigated the excess in the north of Cen A further, by fitting a source model in various energy bands to the northern lobe in which position, extension, and orientation angle of a two-dimensional asymmetric Gaussian were left free to vary. In this case we find a excess of $f_{80-400\text{keV}} = (9.1 \pm 7.8) \times 10^{-4} \text{ ph cm}^{-2} \text{ s}^{-1}$ (3 σ error) at RA = 202.9°, DEC = −40.2°. This is at 1.1° distance from the radio and 1.6° from the *Fermi*/LAT position. In addition, we extracted a spectrum from the best fit position of the northern lobe. The result is shown in Fig. 2

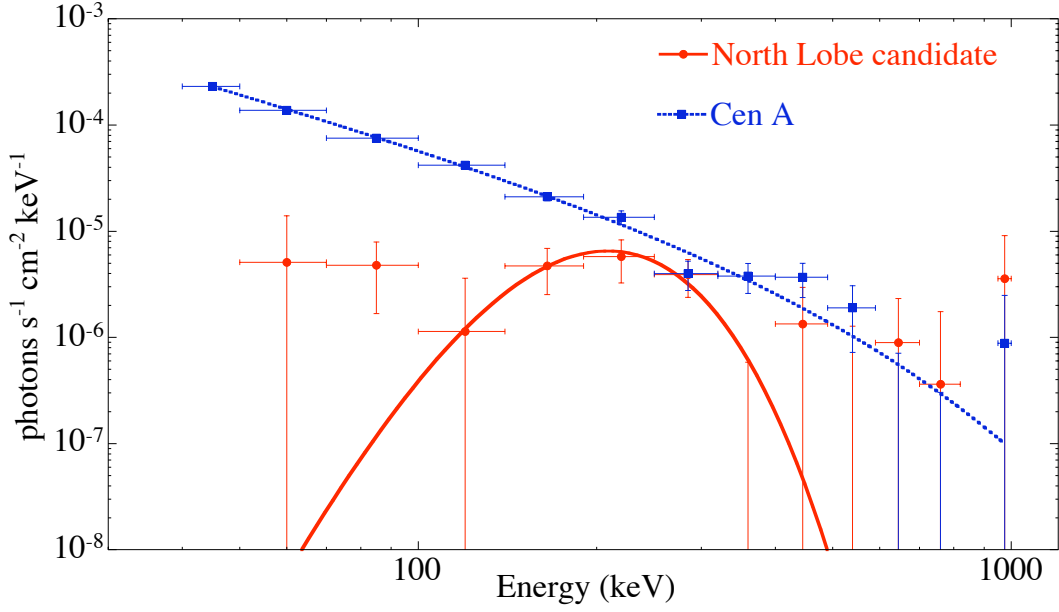


Figure 2: Spectrum of Cen A (blue) and of the north lobe candidate (red) based on the *INTEGRAL*/SPI data.

together with the spectrum of Cen A. It shows that the excess is sustained by three energy bins between 140 keV and 320 keV, with significances larger than 2σ and a flux of $f_{140-320\text{keV}} = (9 \pm 2) \times 10^{-4} \text{ ph cm}^{-2} \text{ s}^{-1}$ ($\sim 4\sigma$). The total flux in the feature between 40–1000 keV is $1.40 \pm 0.5 \times 10^{-3} \text{ ph cm}^{-2} \text{ s}^{-1}$ (2.6σ) which is compatible with the flux obtained assuming a point source, i.e. $(0.9 \pm 0.5) \times 10^{-3} \text{ ph cm}^{-2} \text{ s}^{-1}$. It has to be noted that compared to the point source hypothesis, the flux in Cen A is reduced from $(1.28 \pm 0.05) \times 10^{-2} \text{ ph cm}^{-2} \text{ s}^{-1}$, assuming that the north lobe candidate is a point source, to $(1.19 \pm 0.04) \times 10^{-2} \text{ ph cm}^{-2} \text{ s}^{-1}$, when an extended feature is assumed for the northern lobe candidate.

The 3.5σ signal is too low in order to claim a significant detection at this point. Even if we consider this flux to be a reliable measurement, the hard X-ray lobe emission of Cen A can still be lower, as also other sources in the field can contribute, e.g. in the north 1FGL J1307.0–4030 detected by *Fermi*/LAT, or another so far undetected blazar in the background. Based on the SPI data, it is not yet possible to determine whether the excess we detect is extended or resulting from a point-like source.

If we consider the flux value of $f = 10^{-3} \text{ ph cm}^{-2} \text{ s}^{-1}$ an upper limit, it agrees with the expected energy distribution presented by [14]. At an energy of 300 keV, they expect a contribution to the SED of $\sim 5 \times 10^{12} \text{ Jy Hz}$ in the case of the southern lobe, whereas the upper limit based on the SPI data corresponds to $< 10^{13} \text{ Jy Hz}$. In the case of the northern lobe, the emission expected from the *Fermi*/LAT extrapolation is even lower. Therefore, unless about five times more SPI data will be accumulated on Cen A, the lobes will most likely escape detection at hardest X-rays.

5. Discussion and Conclusion

In the work presented here the Cen A spectrum shows a reflection component when applying a Compton reflection model (*compPS*). Although the reflection strength is comparably low ($R =$

$0.12_{-0.10}^{+0.08}$), it is inconsistent with no reflection on the 3.6σ level. The plasma temperature is $kT_e = 206 \pm 62$ keV with a Compton parameter $y = 0.42_{-0.06}^{+0.09}$.

Extrapolating the cut-off power law model, the `compPS` or the `pextrav` model into the *Fermi*/LAT energy range shows that the inverse Compton component dominating the X-rays cannot be responsible for the gamma-ray emission. Both models predict no detectable flux at energies above 100 MeV. Thus, an additional component, e.g. non-thermal (jet) emission, has to come into play here. This is a well established fact (e.g. [19], [12]) but the perfect match of the Comptonisation model to the *INTEGRAL* data rules out the possibility that the dominant emission in the X-rays is non-thermal, i.e. also arising from the jet as the gamma-ray emission [20]. This is also indicated by the iron line and the Compton reflection hump. The *Fermi* collaboration presented already a model considering the combined thermal inverse Compton plus a non-thermal gamma-ray component to explain the X-ray to VHE emission, although they could not rule out that the X-rays require a non-thermal modeling [12].

The extended emission we see at a low significance level in the *INTEGRAL*/SPI data and which coincides with the northern lobe of Cen A, cannot be detected beyond doubt. *If* this detection is not an artifact, there are several possibilities for its origin. It can be connected to the emission detected by *Fermi*/LAT, although one would expect a stronger emission from the southern lobe in this case. Another possibility is the detection of a background blazar in the hard X-rays. As this source would be a point source, it should show up though also in the hard X-ray data of *IBIS*/ISGRI, which is not the case. It might well be that this hard X-ray feature cannot be verified before the advent of a new generation of MeV telescopes, such as Compton telescopes like *CAPSiTT*, currently under study for ESA's M3 mission call.

References

- [1] Beckmann, V., Soldi, S., Ricci, C., et al. 2009, *A&A*, 505, 417
- [2] Israel, F. P. 1998, *A&ARv*, 8, 237
- [3] Miyazaki, S., Takahashi, T., Gunji, S., et al. 1996, *PASJ*, 48, 801
- [4] Gehrels, N., Chipman, E. & Kniffen, D. A. 1993, *A&AS*, 97, 5
- [5] Steinle, H., Bennett, K., Bloemen, H., et al. 1998, *A&A*, 330, 97
- [6] Rothschild, R. E., Wilms, J., Tomsick, J., et al. 2006, *ApJ*, 641, 801
- [7] Soldi, S., Beckmann, V., Bassani, L., et al. 2005, *A&A*, 444, 431
- [8] Collmar, W., Bennett, K., Bloemen, H., et al. 1999, *Astrophysical Letters Communications*, 39, 57
- [9] Steinle, H. 2010, *PASA*, 27, 431
- [10] Hartman, R. C., et al. 1999, *ApJS*, 123, 79
- [11] Sreekumar, P., Bertsch, D. L., Hartman, R. C., et al. 1999, *Astroparticle Physics*, 11, 221
- [12] Abdo, A. A., et al. 2010, *ApJ*, 719, 1433
- [13] Aharonian, F., et al. 2009, *ApJ*, 695, L40
- [14] Abdo, A. A., et al. 2010, *ApJ*, 719, 1433

- [15] Lubiński, P. 2009, *A&A*, 496, 557
- [16] Poutanen, J., & Svensson, R. 1996, *ApJ*, 470, 249
- [17] Magdziarz, P., & Zdziarski, A. A. 1995, *MNRAS*, 273, 837
- [18] Jean, P., Vedrenne, G., Roques, J. P., et al. 2003, *A&A*, 411, L107
- [19] Johnson, W. N., Zdziarski, A. A., Madejski, G. M., et al. 1997, *Proceedings of the Fourth Compton Symposium*, 410, 283
- [20] Beckmann, V., Jean, P., Lubiński, P., Soldi, S., & Terrier, R. 2010, submitted to *A&A*